# Erosion of the submarine flanks of the Canary Islands

Neil C. Mitchell
Department of Earth Sciences, Cardiff University, Cardiff, U.K.

W. Brian Dade[1]
Department of Earth Sciences, Cambridge University, Cambridge, U.K.

Douglas G. Masson
Southampton Oceanography Centre, Southampton, U.K.

Received 18 November 2002; revised 7 May 2003; accepted 3 June 2003; published 10 October 2003.

[1] Surveying with multibeam echo sounders around old (≫1 Ma) volcanic ocean islands reveals that their submarine flanks contain a strong downslope-oriented ridge-and-valley corrugation, which modifies the original volcanic morphology of lava terraces and cones. By analogy with canyons in other settings, this corrugation was probably caused by channel incision by erosive sedimentary mass flows such as turbidity currents and debris flows. We adapt a method first used in subaerial geomorphology to isolate the erosion depth (exhumation) and apply it to the eroded flanks of the 6–8 Ma Anaga massif of Tenerife. The channels formed around this massif divert around local topographic highs. These highs, which are probably original volcanic cones, are therefore preferentially preserved during erosion, so that their elevations can be used to construct an artificial reference surface. Terrain depth was calculated by subtracting this reference surface from measured bathymetry. Comparison of the terrain depth of the old, eroded submarine flank of Anaga with that of the young, mostly unaltered submarine flank of El Hierro allows us to infer the mean depth of Anaga's submarine erosion, which is ~100 m. Volcanic terrains can be dated by radiometric methods, so they also provide a way of quantifying long-term denudation rates. We infer that submarine denudation of Anaga has occurred at comparable rates to that of subaerial lowlands and much slower than denudation of highlands, illustrated locally by the more extensive erosion of the subaerial Anaga edifice. *INDEX TERMS:* 1815 Hydrology: Erosion and sedimentation; 3022 Marine Geology and Geophysics: Marine sediments—processes and transport; 3045 Marine Geology and Geophysics: Seafloor morphology and bottom photography; 3094 Marine Geology and Geophysics: Instruments and techniques; 1824 Hydrology: Geomorphology (1625); *KEYWORDS:* submarine erosion, denudation, volcanic islands, multibeam echo sounder, turbidity currents, debris flows

**Citation:** Mitchell, N. C., W. B. Dade, and D. G. Masson, Erosion of the submarine flanks of the Canary Islands, *J. Geophys. Res.*, *108*(F1), 6002, doi:10.1029/2002JF000003, 2003.

## 1. Introduction

[2] In the field of subaerial geomorphology, the understanding of erosion is central to understanding the relationships between tectonics, climate and landscape form, and to the understanding of feedbacks between them. Erosion determines the character and rate of sediment flux to basins, and needs to be understood in order to allow climatic and tectonic effects to be deduced from the sedimentary record and from landscape characteristics. Whereas our understanding of the way in which precipitation and tectonic uplift control erosion in subaerial tectonic mountainous landscapes is improving [e.g., *Montgomery and Greenberg*, 2000], the functional controls on submarine erosion are much less clear. This is perhaps not surprising, as a variety of techniques are available to quantify subaerial erosion (exhumation) including thermochronometry, studies of the deposited products of erosion and even surveying over event timescales [*Hartshorn et al.*, 2002], but measuring erosion rates in submarine settings is more challenging.

[3] In this paper, we describe a study of the changes in volcanic island topographic roughness with age, where the roughness of interest here is the downslope-oriented ridges and valleys created by erosive sedimentary flows. The technique that we employ is similar to one used in subaerial geomorphology by *Montgomery* [1994], who calculated erosion depth relative to remnants in an original geological surface. A small complication is that original submarine

[1]Now at Department of Earth Sciences, Dartmouth College, Hanover, New Hampshire, USA.


0148-0227/03/2002JF000003$09.00

volcanic landscapes are already highly rugged, so we quantify the difference in roughness of terrains of different age, rather than assume an original low relief surface. We use volcanic peaks to construct an artificial reference surface which is loosely analogous to the erosional remnants in subaerial geomorphology because these peaks are apparently preserved by erosive flows diverting around them.

[4] Previous work in the Canary Islands is noteworthy for addressing issues associated with the erosion. Sediments recovered during ODP Leg 157 recorded the turbidites and other mass flow deposits formed when Gran Canaria was volcanically active [*Schmincke and Sumita*, 1998]. Such deposits reveal a significant component of upper bathyal foraminifers [*Schneider et al.*, 1998], suggesting that erosion and possibly flow initiation can occur within the upper island flank and involve biogenic material. Some submarine canyons lie seaward of major subaerial canyons [*Funck and Schmincke*, 1998; *Urgeles et al.*, 1999], and *Krastel et al.* [2001a] suggested that sediment laden flash floods may be able to cross the island shelf as hyperpycnal flows to feed submarine canyons in such locations. Sedimentary bedforms, indicating down-slope passage of sedimentary mass flows, have been imaged on the upper chute of the Icod debris avalanche of Tenerife using deeply towed side scan sonar [*Watts and Masson*, 2001] and in the upper southwest flank of El Hierro using multibeam sonar [*Masson et al.*, 2002]. We agree with *Krastel et al.*'s [2001a] interpretation that the canyons studied here formed in the submarine environment as there is little evidence for a depressed ancient abrasion platform if these were formed subaerially and later subsided [*Mitchell et al.*, 2002]. We also favor their formation by downslope eroding flows [*Krastel et al.*, 2001a], as the alternative, upslope growth by retrogressive landsliding initiated near the base of the slope [e.g., *Farre et al.*, 1983], seems unlikely given that the islands typically have their lowest gradients at their bases [*Mitchell et al.*, 2002].

[5] A prominent feature of the Canary islands is that they have experienced large-scale landslides (commonly in the form of debris avalanches), probably during their most volcanically active phases [*Krastel et al.*, 2001b; *Masson et al.*, 2002; *Carracedo et al.*, 1999]. Their deposits cover 30–50% of the island submarine flanks [*Mitchell et al.*, 2002] and their volumes are significant, e.g., >1000 km$^3$ for the Tenerife debris avalanche deposits [*Cantagrel et al.*, 1999]. The Anaga and El Golfo debris avalanche features are marked in Figure 1, showing smooth chutes and (in the case of El Golfo) an embayment on land which marks the avalanche headwall. We make a distinction between this large-scale sedimentary process and those erosive processes which are responsible for carving the gullies and canyons on the island flanks, addressed in this study. Since at least part of the superficial flank erosion probably occurs by small-scale landsliding and avalanching, this distinction may seem arbitrary but there appears to be a division of these scales of process here.

[6] This paper is structured as follows. We first outline the geology of El Hierro and the Anaga massif (Tenerife), which suggests that these are comparable volcanic edifices. We describe the data and method applied to quantify terrain depth, before making comparisons with the subaerially eroded volume of Anaga. We then speculate on the likely timescale and rate of the erosion and relate our results to submarine erosion more generally.

## 2. Geological Background to the Anaga Massif (Tenerife) and Western El Hierro

### 2.1. El Hierro

[7] The western promontory of El Hierro has been described [*Carracedo*, 1994] as a ridge formed by eruptions from a volcanic rift zone, marked by fissures and aligned eruptive vents overlying dike swarms, which overprint a basaltic carapace [*Guillou et al.*, 1996]. Offshore, multibeam sonar data show that volcanism has been more broadly distributed than observed on land, with volcanic cones observable across a broad sector [*Gee et al.*, 2001; *Mitchell et al.*, 2002] (Figure 1b). At 2–3 km depth, the island flanks contain lobate lava terraces.

[8] The age of the westerly submarine extension of El Hierro is most probably $\ll$1 Ma. *Carracedo et al.* [1999], based on K-Ar dating and magnetostratigraphy [*Guillou et al.*, 1996], describes growth of the centrally located El Golfo volcano around 550–176 ka and later rift volcanism continuing to 134 ka which may have both caused significant subaerial growth on the western limb of the island. They show further volcanism continuing there from 134 ka to historical times. Given that the subaerial limb has been historically active [*Carracedo*, 1994], the westerly submarine terrain is unlikely to be of any significant age compared to Anaga. It is most probably much less than 1 Ma, perhaps as young as 100 ka.

[9] We use the northeast submarine extension of El Hierro as a second 'zero age' terrain in the following analysis in order to help characterize uncertainty in the method, so it is also described here. The area is not shown but is morphologically similar to westerly El Hierro [*Gee et al.*, 2001; *Mitchell et al.*, 2002]. The bulk of the northeast sector of the subaerial island was built by the Tinor volcano at 0.88–1.12 Ma of largely basaltic lavas [*Gouillou et al.*, 1996; *Carracedo et al.*, 1999]. Younger rift zone volcanics have left a similar distribution of eruptive vents to those of westerly El Hierro [*Carracedo et al.*, 1998; *Urgeles et al.*, 1997] and one very young (25 ka) $^{14}$C age has been recorded [*Gouillou et al.*, 1996]. This sector therefore has an older base compared to westerly El Hierro. The submarine volcanic morphology appears similar to westerly El Hierro and hence of similar age but ages up to 1.12 Ma cannot be ruled out.

### 2.2. Anaga

[10] The Anaga massif (Figure 1a) is an old shield volcano, with the younger Las Cañadas stratovolcano and rift zone (Dorsal) volcanics grown later on its western side [*Ancochea et al.*, 1990]. A number of observations suggest that a volcanic rift zone was centered on the present north side of the island (Taganana area located as the black region in Figure 1a) that was oriented northeast-southwest. *Rodriguez-Losada et al.* [2000] describe highly altered, brecciated and eroded dikes, forming a basal series typical of the Canary islands. These dikes form an intense swarm, locally occupying 100% of outcrop and strike northeast-southwest. The area lies slightly north of the edifice center

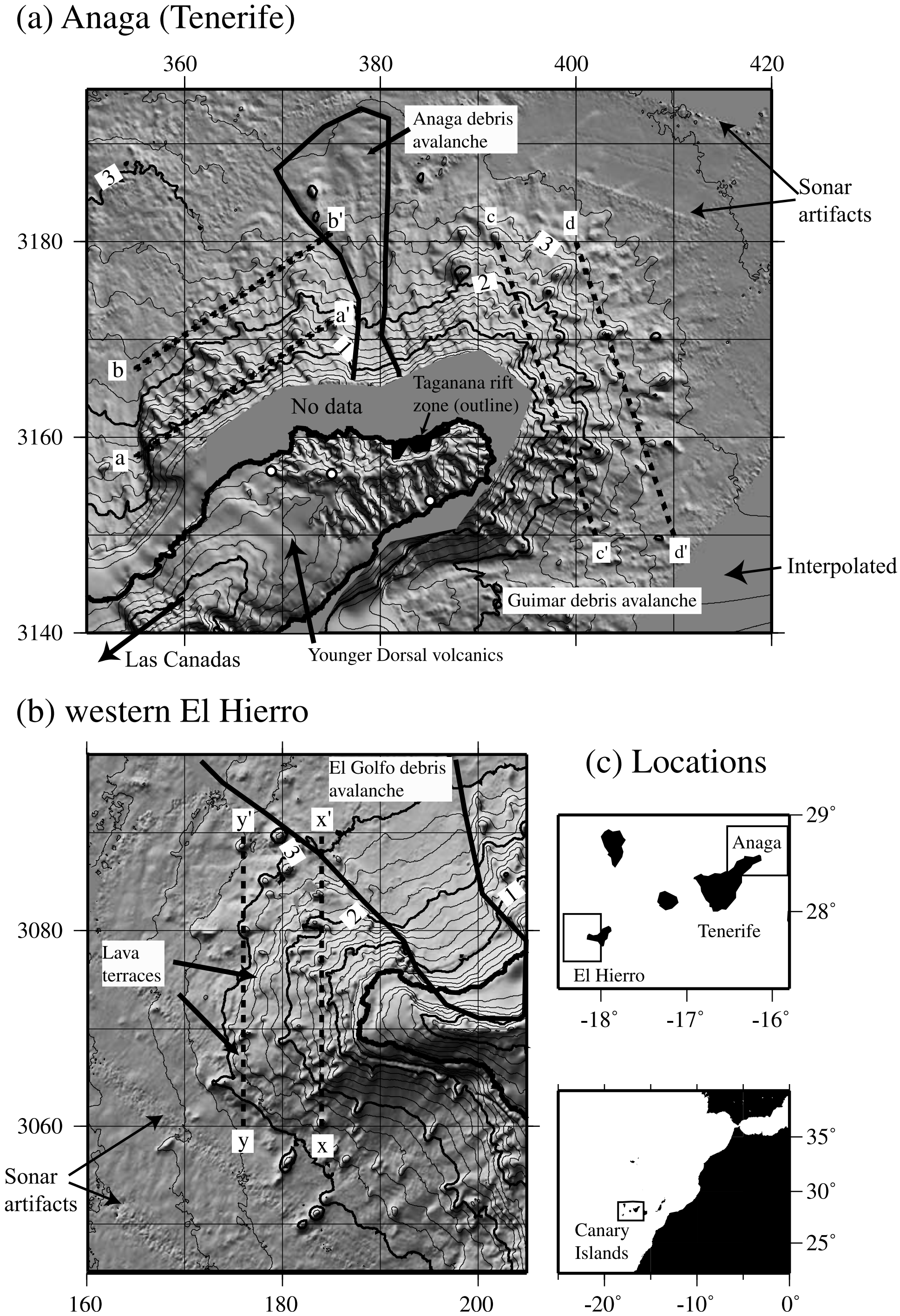


**Figure 1.** Bathymetry of the two Canary island areas considered here. (a) The Anaga massif of Tenerife. (b) The western promontory of El Hierro. (c) The location of the Canary Island data sets shown in Figures 1a and 1b. The coordinates in Figures 1a and 1b are Universal Transverse Mercator (UTM) zone 28 distances in km. The dashed lines locate sections shown in Figure 7. The topographic maps are shown with an artificial illumination from the northwest. Contours are every 200 m with depths annotated in km.

defined by the island shelf break (Figure 2) as expected if this were part of the original central volcanic rift zone. Furthermore, large positive Bouguer gravity anomalies [*Arana et al.*, 2000] occur on the north side of the massif, consistent with an intrusive complex.

[11] The Anaga massif has been dated (K-Ar) onshore as 3.6–6.5 Ma [*Ancochea et al.*, 1990] and offshore as 6 Ma by seismic correlation with ODP Site 953 [*Funck and Lykke-Andersen*, 1998]. More accurate Ar-Ar dates [*Thirlwall et al.*, 2000] are older for a given location and suggest that

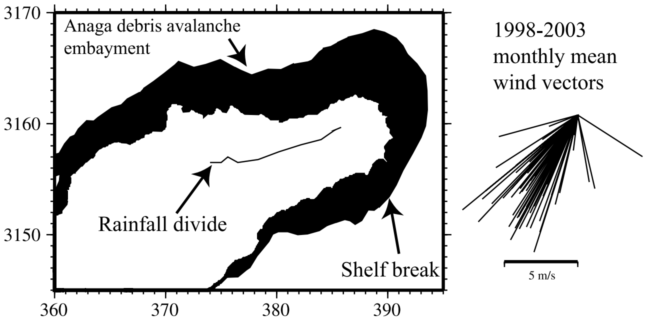


**Figure 2.** Geometry of Anaga's abrasion platform of Tenerife derived from *Teide Group* [1997]. The locations of features are corrected for position errors so as to be consistent with the multibeam data in Figure 1a. The coordinates are UTM zone 28 distances in km. The wind vectors shown on the right are monthly averaged observations of surface wind for January 1998 to March 2003 for the area 28°–30°N, 16°–18°W. These data were collated from marine reports by the NOAA National Centers for Environmental Prediction (Climate Diagnostics Center, Boulder, Colorado).

volcanism was more persistent. These dates include (open circles in Figure 1a) 8.05 ± 0.14 Ma (northwest area), 5.69 ± 0.06 Ma (southeast coast), and 4.23 ± 0.08 Ma (western summit area). These represent the different volcanic sequences and suggest that the edifice approached sea level from around 8 Ma onward. The island probably continued growing in a protracted shield phase until 6 Ma (from the seismic correlation [*Funck and Lykke-Andersen*, 1998]). We assume an age of 6 Ma for the submarine flanks.

## 3. Data and Observations

[12] The bathymetric data from the Canaries (Figures 1 and 3) were acquired using a Simrad EM12S multibeam sonar [*Hammerstad et al.*, 1991] during two cruises of RRS *Charles Darwin* in 1993 and 1997 [*Masson et al.*, 2002; *Watts and Masson*, 1995] and a cruise of B.I.O. *Hesperides* (Crescent-94 [*Urgeles et al.*, 1997]). Note that the topography and coastline shown in Figure 1a have a small position error which is corrected in Figure 2. Medium grey or excessively smooth bathymetry in the figures indicates missing or interpolated regions, respectively. As marked at top right in Figure 1a, the outer beams of the sonar can have noisy readings due to acoustic or motion sensor problems. These affect the appearance of data in flat regions but are minor compared to the scale of geological features around the island slopes studied here.

[13] The data reveal an asymmetric effect of subaerial and submarine erosion of the Anaga massif; the north subaerial slopes of the island are steeper than those to the south so that the rainfall divide lies north of the island's center (Figure 1a). The rainfall divide shown in Figure 2, however, almost exactly bisects the submarine edifice as defined by the shelf break so its location may have been inherited from the original volcano topography. For comparison, the modern trade winds are shown in Figure 2. These have been stable over the period of historical records [*Michelchen*, 1981], and whereas there is pollen evidence for their varied vigor during alternate glacial and interglacial periods, they have probably had a stable direction over 150 kyr and longer periods [*Hooghiemstra*, 1989; *Sarnthein et al.*, 1982]. The greater width of the abrasion platform and steeper subaerial slopes on the north side of the island are therefore both consistent with trade winds from the northeast persistently leading to greater precipitation on the north slopes and more powerful sea swell from the northeast. The average shoreline retreat (4–5 km to the north and 3–4 km to the south) is broadly consistent with *Menard*'s [1983] rates of shelf growth in the Canaries (0.6–0.7 km/Myr) and the 6 Ma age of Anaga [*Ablay and Hurlimann*, 2000].

[14] Figure 4 shows the channels in the island flanks interpreted by tracing depressions. Channels are downward converging in the upper flanks but become downward diverging in the lower flanks. This transition occurs at roughly 2500 m depth where the local slope magnitude declines below 7° (Figure 5a, right, showing the median slope (bold) for the area in Figure 3c). The cross-sectional geometries of channels at this depth show no evidence of flat floors typical of aggradation so this transition is probably caused by forced divergence of sedimentary flows by the irregular topography rather than a change to aggradational flow behavior.

[15] The diversion of channels around local highs is important for our technique described below and is highlighted by the circles in Figure 6. Channels can be seen formed around local highs (e.g., one 50 m deep channel at A in Figure 6), or there can be a more subtle diversion of the channel path (e.g., at B). We interpret this as evidence that erosive sedimentary mass flows, probably turbidity currents and debris flows, were deflected by the original topography [*Pratson et al.*, 1994] and therefore the original peaks in the terrain are preferentially preserved compared to the topographically lower areas between them.

[16] Channels have sharp V-shaped cross sections in the upper flanks, in particular for section c–c′ in Figure 7b. The area around (397E, 3168N UTM km) is a broad amphitheater analogous to those of the upper New Jersey continental slope which *Pratson and Coakley* [1996] interpreted as enlarged by repeated small-scale landsliding. Sedimentary mass flows initiated by slope failure in the steep upper flanks of the island may therefore have caused part of the observed erosion in addition to the hyperpycnal flows mentioned earlier. There is some evidence for channels having greater vertical relief higher in the flanks than lower down, which would be consistent with the greater flow power of turbidity currents associated with the steeper gradient (more than doubling of specific flow power with gradient from 6° to 11° (Figure 5a) from this factor alone). This is not reflected in the terrain depth also shown in Figure 5a probably because of variations in the original volcanic geomorphology.

[17] Where the base of the edifice reaches the island's archipelagic apron, the sharp crests of interfluves can be seen continuing away from the edifice and becoming progressively buried by abyssal sediment. The channels may have been active earlier in Anaga's history but now the edifice base is an area of deposition rather than erosion,

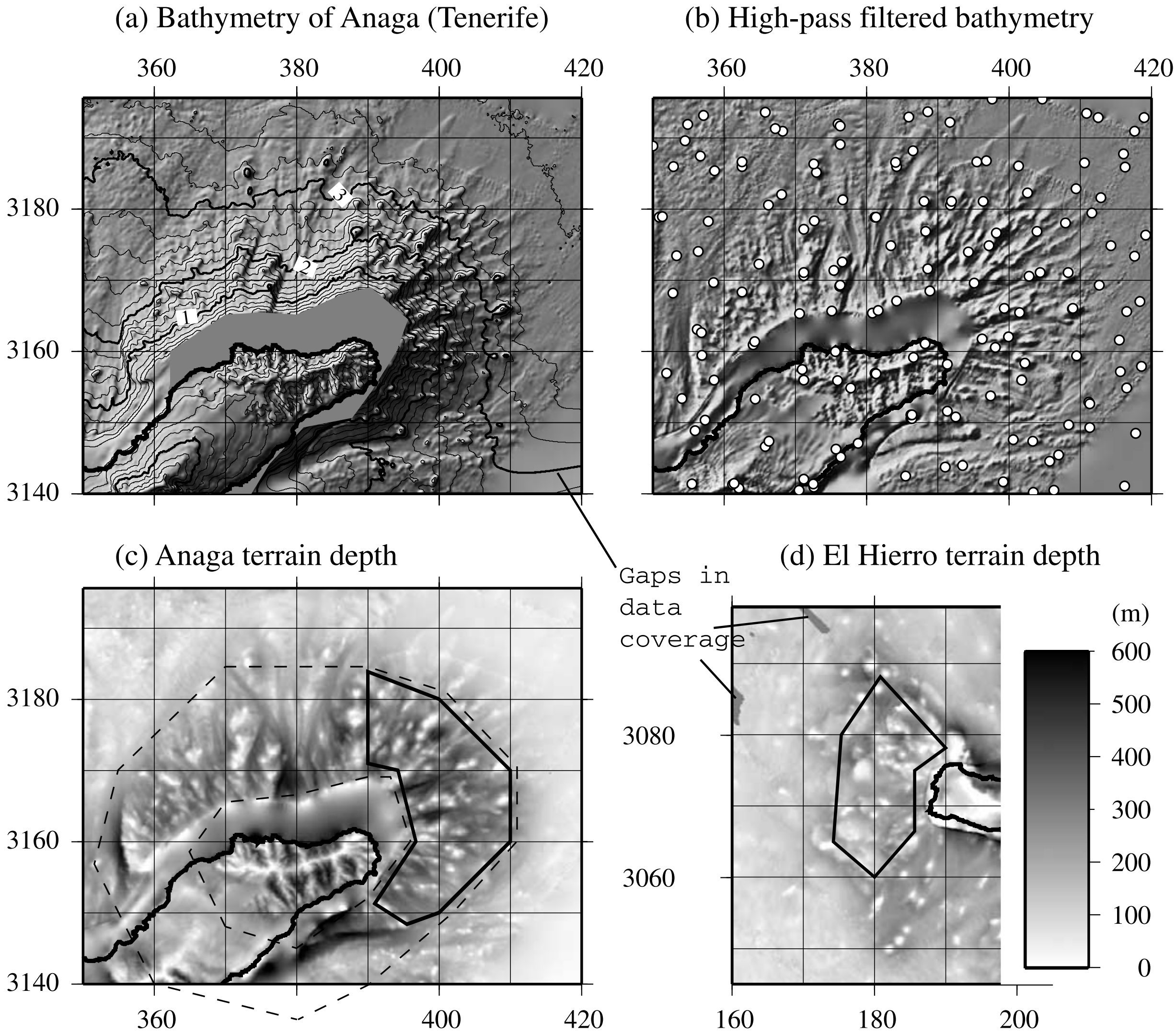


**Figure 3.** (a) The Anaga massif in east Tenerife. Contour interval every 200 m and annotation in kilometers below sea level. The coordinates are UTM zone 28 distances in km. (b) High-pass-filtered version of Figure 3a shown as a shaded-relief image. Open circles locate the topographic peaks in the data set. (c) Terrain depth after subtracting a surface through the peaks in Figure 3b. The dashed lines represent the model original Anaga submarine flank area. (d) Terrain depth for El Hierro calculated as for Anaga. Notice the shallower depths in this terrain (lighter grey) compared to those for Anaga. Both Figures 3c and 3d have the same gray scaling and the bold polygons outline areas used to calculate eroded volume. Bathymetry data in Figures 3a and 3b are shown as in Figure 1a.

leaving only interfluve ridges observable. This is confirmed by low acoustic backscatter in sonar data [*Masson et al.*, 2002], which implies that coarse material in the lower gullies is buried with fine sediment to at least a few meters in order to attenuate the sonar's 13 kHz frequency [*Mitchell*, 1993]. Topographic cross sections also show a more subdued terrain near to the edifice base (lower curves of Figures 7a and 7b). This present inactivity coupled with the growth of the shelf described earlier suggests an interesting connection with the submarine erosion. The hyperpycnal flows produced by floods [*Krastel et al.*, 2001a] would have been most effective when the island was young, lacking a shelf and with steep subaerial slopes. As the shelf grew by coastal abrasion and subaerial erosion, the submarine canyons would have been progressively disconnected from their fluvial sources of hyperpycnal flows, in particular those to the northeast (Figures 4 and 2).

[18] Figure 7c shows two sections across the western flank of El Hierro, revealing a different topographic character to Figures 7a and 7b. The terrain is generally smoother with more rounded hill crests and less sharply defined valleys. Occasional peaks occur, many of which are isolated cones.

## 4. Method for Comparing Terrains

[19] The method is illustrated in Figure 8. We assume that the volcanic peaks of the terrain (highlighted by circles in Figure 8) remain after erosion. The technique involves forming an artificial reference surface through the peaks

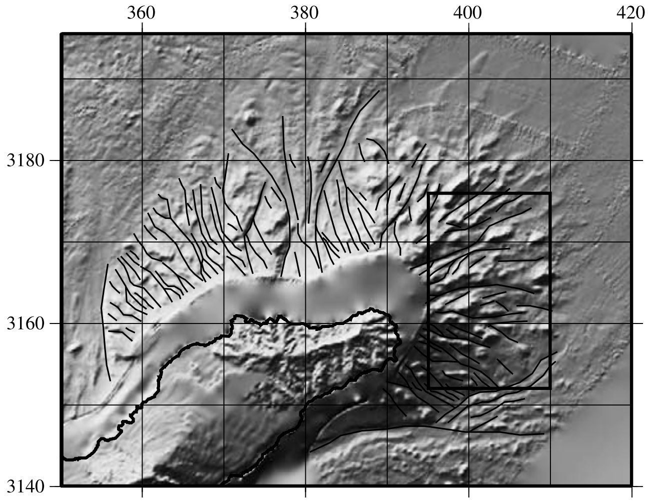


**Figure 4.** Interpreted canyon chutes on the submarine flanks of Anaga (Tenerife). Chutes are down-slope converging on the upper slope and down-slope diverging on the lower slope. The area outlined is shown in Figure 6. The topographic map is shown with an artificial illumination from the northwest, and coordinates are UTM zone 28 distances in km.

of the terrain (dashed line in Figure 8) and then measuring the terrain depth $H$ relative to that reference. $H$ should be greater for an eroded terrain (lower curve in Figure 8) than one before erosion, so comparing the calculated $H$ of two terrains of different age should constrain relative depth of erosion. The calculation of $H$ (local relief) ignores other changes to the regional elevation, such as caused by subsidence [*Watts et al.*, 1997], as we are interested in isolating the exhumation by erosion.

[20] The key assumptions are that (1) volcanic peaks of the terrain remain after erosion, (2) that the two compared terrains had a similar original topographic roughness and (3) that there is a spatial scale over which we can identify peaks in the terrain and erosion creates channels that are everywhere narrower than this scale. Assumption (1) is supported by the diversion of channels mentioned earlier, but some erosion of the original cones could lead to our eroded volume being an underestimate. Assumption (2) is more difficult to verify except to say that we see no indication in the subaerial geology to suggest that they were greatly different. We calculated terrain depth from a third young terrain (northeast El Hierro) to represent the effect of uncertainty in this assumption. For assumption (3) we note that the broadest channels in the data set lie to the northeast of Anaga (identified in Figure 7b). We measured 5 km between interfluve ridges here and used this for the separation lengthscale, but also repeated the analysis with other lengthscales to characterize the uncertainty.

[21] Figure 3a shows the Anaga bathymetry. Figure 3b shows the data after high-pass filtering with a spatial cutoff of 5 km. Local peaks in Figure 3b were located within 5 by 5 km squares and are shown by the open circles. We fitted a taut surface through these peaks to form an artificial reference surface, equivalent to the dashed line in Figure 8. We then subtracted this reference surface from the filtered data to effectively create a map of $H$ (Figure 3c). Figure 3d shows the data for El Hierro after the same sequence. Note that we ran this simple algorithm over the whole area so the peaks identified in Figure 3b include outer beam sonar noise in areas of flat bathymetry (northeast of map), blocks of the Anaga debris avalanche and subaerial parts of the island. However, we use terrain depth only from the area outlined in Figure 3c in the following calculations. An alternative method might involve manually identifying peaks before forming the reference surface, but it may be difficult to prevent subjectivity because peaks can be modified by the erosion.

## 5. Results

[22] Figures 3c and 3d show that the Anaga edifice has a greater terrain depth than western El Hierro. Figure 9 shows histograms of the data outlined in Figures 3c and 3d. The histogram for El Hierro can be made almost to coincide with that for Anaga if it is rescaled (dashed line in Figure 9) by multiplying depths by 1.55 and dividing the histogram counts by 1.55 to maintain histogram area. Multiplying the relative change implied by the rescaling factor (0.55) with the mean depth anomaly $H$ of El Hierro (182 m), we

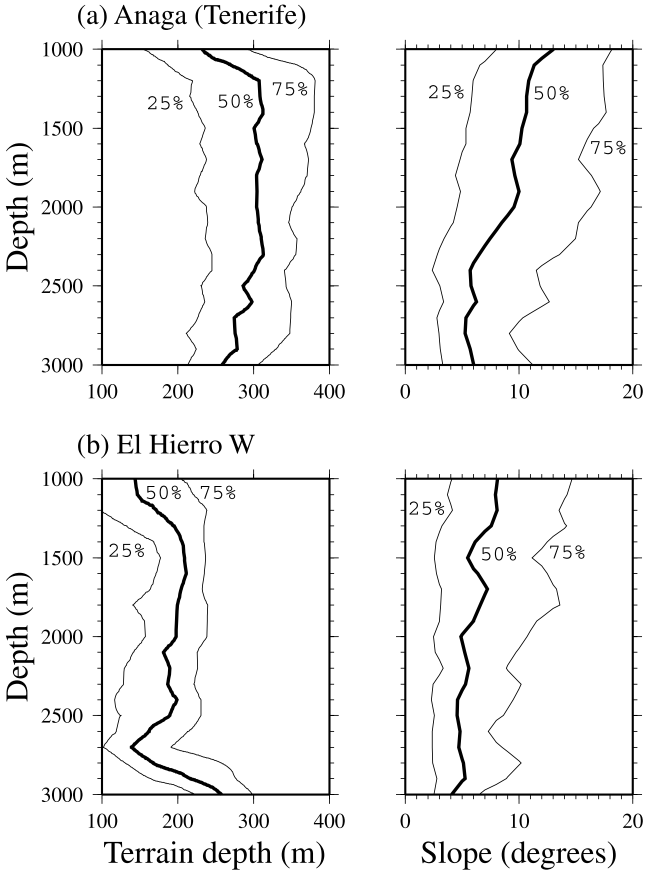


**Figure 5.** The graphs show the median average and interquartile range (values corresponding to 25% and 75% of the cumulative histogram) of terrain depth and local maximum slope [*Mitchell et al.*, 2002]. (a) Graphs for east Anaga corresponding to the area outlined in Figure 3c. (b) Graphs for El Hierro west outlined in Figure 3d.

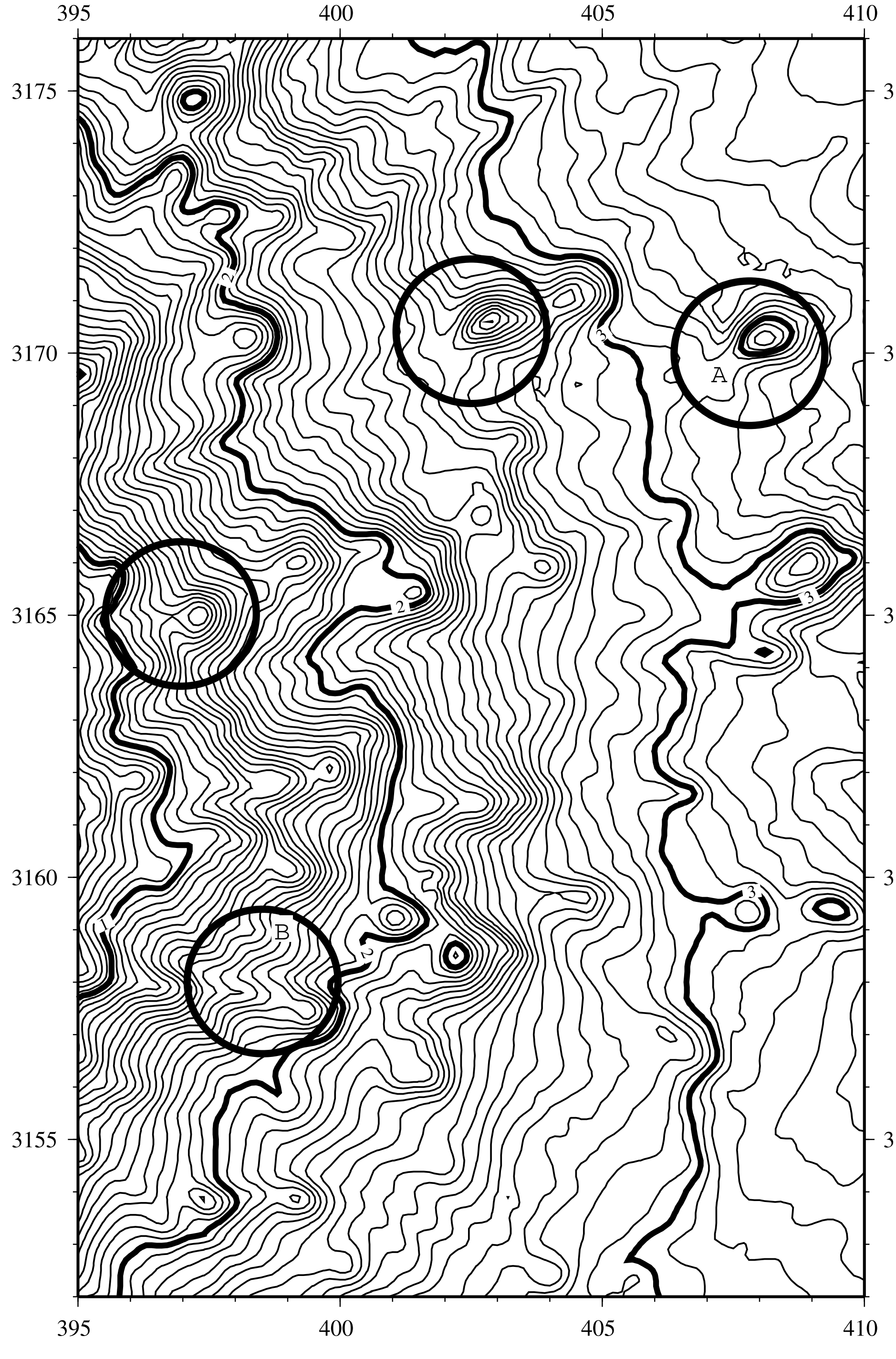


**Figure 6.** Enlargement of multibeam sonar bathymetry data for east Anaga (Tenerife) showing hills and other topographic promontories interpreted as original volcanic cones. Topographic furrows can be seen commonly diverting around these hills, such as where highlighted by circles. We interpret these furrows as channels eroded by sedimentary mass flows such as turbidity currents and debris flows. The channel diversions around the cones suggest that cones are preferentially preserved during erosion. The map coordinates are UTM zone 28 distances in km. Contours are every 50 m, and contour values are depths in km.

infer that Anaga has been lowered by 100 m on average. Locally the lowering has been 200–300 m within the deepest gullies in Figure 7b.

[23] We estimated a total eroded volume for the submarine flanks by subtracting the volume in Figure 3d (46 $km^3$) from the volume in Figure 3c (121 $km^3$), rescaled to allow for their different surface areas. This volume (43 $km^3$) was then rescaled to represent the volume eroded from the flanks of the whole edifice, which we suspect had an original surface area roughly three times that outlined in Figure 3c as

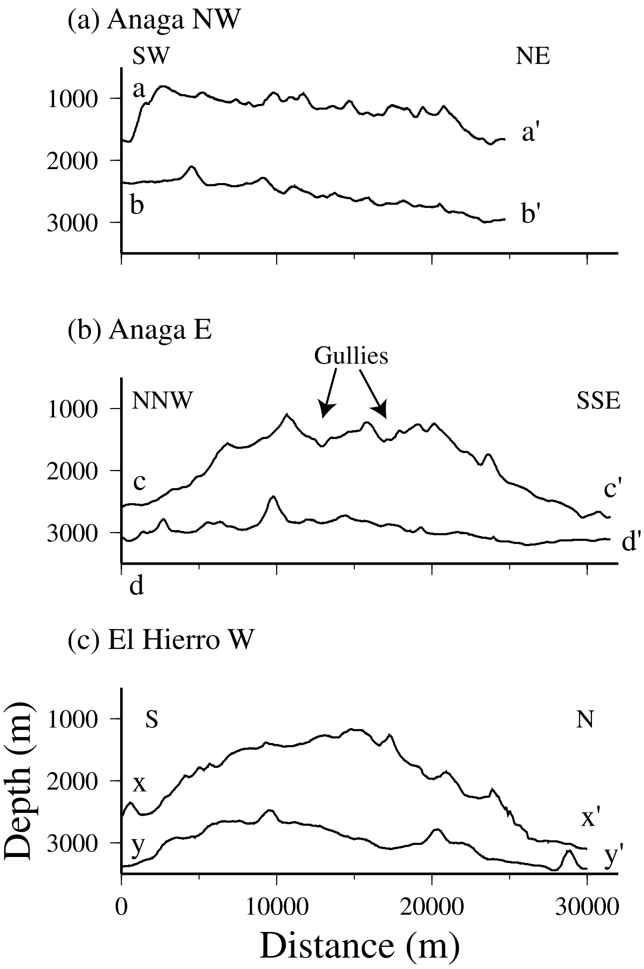


**Figure 7.** Cross sections over the eroded older flanks of the Anaga massif compared to the less eroded flanks of El Hierro (sections located in Figure 1). (a) Cross sections along the northwest flank of the Anaga massif showing a shallow incision of topography. (b) Cross sections across the east flank of Anaga including (upper section) two deep V-shaped eroded channels. (c) Cross sections across the west flank of El Hierro island. Note the more rounded, smooth morphology compared to Figures 7a and 7b.

illustrated by the dashed line. The total volume eroded is therefore 130 ± 70 km$^3$, where the uncertainty was calculated from the uncertainties of (1) choice of reference terrain (±58 km$^3$) and (2) choice of filter width for the high-pass filtering (±38 km$^3$). Uncertainty 1 was estimated by repeating the above procedure but using the northeast flank of El Hierro, which the earlier literature review suggests is relatively young (0–1 Ma) and superficially similar to westerly El Hierro (this yields an eroded volume of east Anaga of 24 km$^3$ or 72 km$^3$ if scaled to the whole flank area). Uncertainty 2 was estimated by repeating the procedure illustrated in Figure 3 but with different filter width. Figure 10 shows the volume outlined in Figure 3c with varied $F$ (equal to twice the effective cutoff scale of the filter). The uncertainty (±29%) was given by the range in eroded volume over $5 < F < 15$ km. Further uncertainties originate from lack of knowledge of the original submarine flank area of the island now buried by the younger Dorsal volcanics and indeed whether the Anaga massif was even an isolated edifice. These cannot be evaluated numerically and hence the results are considered to represent a 'model' erosion volume extrapolated from the east area of Anaga (i.e., the volume eroded if the edifice had this size). It is also a model volume in the sense that the Anaga debris avalanche (and other unknown similar structures beneath Dorsal) are not included.

[24] The volume removed by subaerial erosion and coastal abrasion was estimated as follows, first estimating the likely original volcano altitude. The altitudes of the Cumbre Vieja (La Palma) and Dorsal (Tenerife) linear ridges are ~1800 and ~1400 m, respectively. To estimate an original altitude for Anaga, we scaled these altitudes using the difference in width of the islands at sea level of Cumbre Vieja and Dorsal (both ~14 km) and the width of the abrasion platform of Anaga (~16 km). This gives altitudes of 2060 and 1600 m, respectively. *Vogt and Smoot* [1984] compiled volcanic island altitudes and showed a variation of ±50% in peak altitude for a given island area. We therefore chose a most likely Anaga altitude of 1800 m but repeated the following with this altitude varied by ±50% to conservatively represent uncertainty. Figure 11 shows a topographic model constructed using the 1800 m altitude interpolated to the multibeam bathymetry.

[25] The present-day topography (Figure 1a) was then subtracted from this model to yield an eroded volume of 150 km$^3$ (50–260 km$^3$, an uncertainty range arising from the ±50% altitudes). Because the volcano likely went through protracted phases of growth and erosion of subaerial material, these volume estimates are most likely minima. Furthermore, the subaerial eroded volume includes the effects of the Anaga debris avalanche (and potentially other unresolved landslides), whereas the submarine erosion estimate excludes this contribution.

[26] Although the volume of the Anaga debris avalanche is unknown, we note that several Canary Island debris avalanche deposits have similar volumes to the above subaerial and submarine erosion volumes. For example,

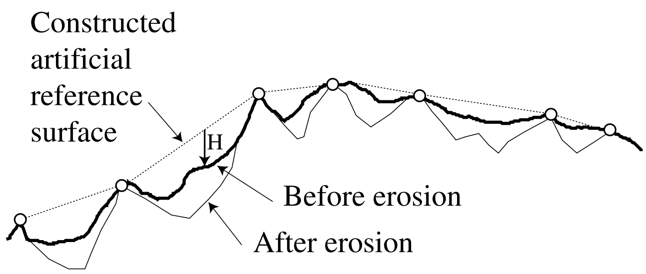


**Figure 8.** Method adopted in this paper to resolve changes in the terrain depth relative to an artificial reference surface (dashed line in figure) constructed through local topographic peaks. Because channels divert around the peaks (Figure 4), changes in terrain depth ($H$) relative to the constructed reference surface reveal the amount of erosive lowering. This is carried out in practice by calculating $H$ for two terrains of different age. The erosive lowering is then revealed by differences in the statistical characteristics of $H$ between them.

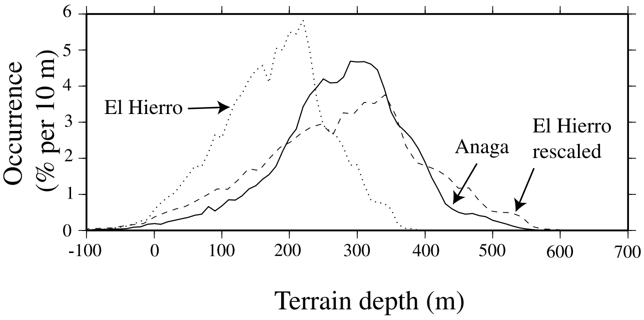


**Figure 9.** Histograms of the depth anomaly (*H*) of the two areas in Figures 3c and 3d (solid and dotted lines, respectively). Zero depth anomaly corresponds to the white shading in Figures 3c and 3d. The dashed line shows the histogram for El Hierro rescaled so that it approximately coincides with the histogram for Anaga. The rescaling was achieved by multiplying depths of the histogram by 1.55 and dividing the corresponding occurrences by 1.55 to conserve the histogram area. Given that the mean terrain depth of El Hierro is 182 m, this correspondence implies that Anaga has been eroded to an average depth of 100 m (i.e., the mean depth is increased by 182 times 0.55).

*Urgeles et al.* [1997, 1999] estimated volumes of 150 and 95 $km^3$ for the El Golfo (El Hierro) and Cumbre Nueva (La Palma) debris avalanches, respectively. The area of the Anaga debris avalanche deposits, >400 $km^2$ [*Masson et al.*, 2002], is larger than half that of the Cumbre Nueva deposits (780 $km^2$ [*Urgeles et al.*, 1999]). We therefore suspect that the Anaga deposit volume is roughly comparable to that of the Cumbre Nueva.

[27] The above results show that the model submarine eroded volume is similar within uncertainties to the subaerial eroded volume and to the likely volume of the Anaga debris avalanche deposit. Therefore, although coastal and subaerial erosion and the large-scale landslides produce a more prominent effect on the edifice's morphology, they occur over smaller regions than the superficial submarine erosion and these different eroded volume estimates turn out to be comparable.

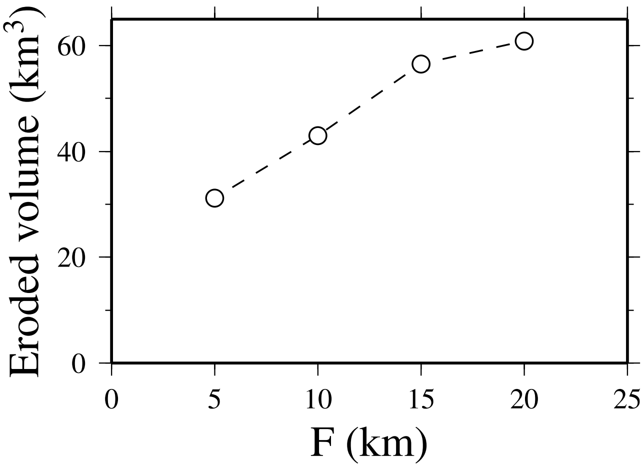


**Figure 10.** Dependence of the inferred submarine eroded volume of east Anaga on the high-pass filter width *F.* The volume shown is the integrated volume of Figure 3c minus the volume of Figure 3d scaled to the area of Figure 3c.

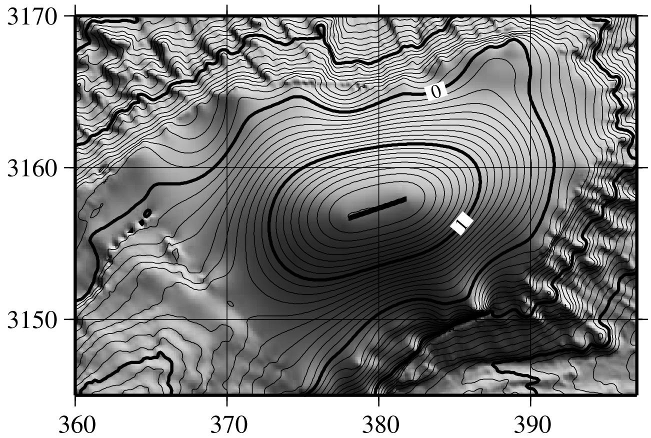


**Figure 11.** A topographic model of the preerosion edifice of Anaga, consisting of a linear volcanic ridge bisecting the topography of the submarine edifice. (The topography of the Dorsal volcanics is left in as this is removed when the present eroded island topography is subtracted.)

## 6. Discussion

[28] Submarine denudation rates, as far as we are aware, have not been systematically addressed in the literature. Qualitatively, the data in Figure 1 indicate that over the lifetime of the edifice, the submarine denudation has occurred at a slower average rate than the subaerial and coastal erosion because the subaerial edifice has lost a substantial altitude (probably >1000 m over the Taganana rift zone) compared to only 100 m offshore. We note that many submarine landscapes imaged with multibeam sonar also show less apparent denudation offshore compared to their adjacent subaerial mountain scapes. For example, multibeam data from offshore Los Angeles show that submarine slopes around the Palos Verdes Peninsula (a late Pleistocene anticline associated with the strike-slip faults) are incised, though less degraded than the subaerial headland itself [*Marlow et al.*, 2000].

[29] A rough estimate of the mean erosion rate is provided by assuming that the main period of erosion occurred over 2 Myr. This period probably occurs during or shortly after the main volcanic building of an edifice. The 2 Myr timescale is based on the age range of volcaniclastic sedimentary mass flow deposits in ODP Site 953 originating from Gran Canaria's emergent phase lasting $\leq$1 Myr [*Carey et al.*, 1998], typical 1 Myr duration of main shield building in volcanic ocean islands [*Clague and Dalrymple*, 1989] and the range of dates on Anaga [*Thirlwall et al.*, 2000]. Furthermore, the northwestern flank of La Palma is now incised [*Urgeles et al.*, 1999] and is <2 Ma [*Carracedo et al.*, 1999]. This timescale yields a mean denudation rate of 50 m/Myr; however, if erosion occurred over the longer 6 Myr lifetime of the edifice flanks [*Funck and Lykke-Andersen*, 1998], the mean erosion rate was 17 m/Myr.

[30] Denudation rates of 17–50 m/Myr are comparable to denudation rates of subaerial lowlands calculated over similar timescales but are, as would be expected, much

slower than long-term denudation rates of subaerial mountain regions, which are ~1000 m/Myr [*Selby*, 1993]. In contrast, the incision of mid-ocean ridge fault escarpments is much slower; from data of *Tucholke et al.* [1997] we deduce a local vertical incision rate of 1.5–2.5 m/Myr over a 20 Myr timescale. Therefore, whereas the rates we have calculated are by no means accurate, they do seem to be reasonable.

[31] The finding that significant volumes are eroded from the island flanks also has implications for efforts to infer an island's volcanic evolution by studying sedimentary cores [e.g., *Masson*, 1996; *Schmincke et al.*, 1995]. Deposits are likely to have a significant component derived from the flanks. In one model [*Clague and Dalrymple*, 1989], the evolution of an oceanic island is believed to involve commonly a shield tholeiitic phase, followed by a later alkalic rejuvination phase building more limited volumes. Thus erosion of the submarine regions can incorporate preferentially the earlier shield material, whereas the subaerially originating material can include the later alkalic phase, potentially complicating the interpretation of drill core data.

[32] The asymmetry in the erosion of Anaga's abrasion platform implies a potentially interesting connection with the history of the submarine canyon incision. Greater rainfall in the north associated with the northeast trade winds may have led to more frequent and intense floods on the north side of the edifice. Initially, hyperpycnal flows generated by these floods will have been most erosive to the submarine canyons on the north side, but with time they may have become less erosive as the abrasion platform grew and as the submarine canyons became more distant from their hyperpycnal sources. The details of this evolution depend on a number of unknown factors affecting flows over this period, such as the delivered solid load and the diversion or dilution of hyperpycnal flows by the shallow Canary Current. The erosive potential of the flows will also have varied over eustatic sea level cycles with subaerial and submarine canyons potentially becoming temporarily reconnected during low stands. Future investigations may consider addressing this evolution by taking cores around a structure such as Anaga. Such cores should catalogue the deposition of submarine and subaerial materials at the base of the canyons and reveal whether the history of erosion progressed around the edifice as proposed here.

## 7. Conclusions

[33] Our analysis of the difference in topographic roughness between the submarine flanks of Anaga and El Hierro implies that the erosion has deepened the terrain by 100 m on average and locally 200–300 m in the deepest channels. The model total volume eroded from the submarine flanks is $130 \pm 70$ km$^3$, a figure that overlaps with our estimates of the subaerial eroded volume of 150 km$^3$ (uncertainty range 50–260 km$^3$). Therefore, although the subaerial erosion produces a more pronounced effect on the edifice's morphology, the submarine erosion occurs over a larger area and removes a comparable volume within our uncertainties. Subaerial and coastal erosion have been asymmetric with greater erosion leading to Anaga's abrasion platform being 1 km wider to the north than to the south, an effect of trade winds originating from the northeast. The geometry of the platform implies a potentially interesting connection with the history of the submarine canyon incision. Submarine erosion should have initially been more intense in the north because of rivers more frequently feeding hyperpycnal flows, but as the abrasion platform grew there may have been a progressive disconnection of submarine channels in the north from their erosive sources.

[34] Our best estimate of the timescale of the erosion is 2 Myr and maximum 6 Myr. Using these values, the mean rate of denudation was 17–50 m/Myr. These denudation rates lie between much slower rates of deep-ocean mid-ocean ridge fault escarpments and the faster rates of subaerial mountain environments, but are comparable to the moderate rates of subaerial lowlands. These submarine landscapes therefore 'age' at a moderate rate. These results demonstrate the potential for quantifying erosion of submarine landscapes more generally, which could ultimately lead to a better understanding of the functional controls on submarine erosion to compare with those of subaerial geomorphology.

[35] **Acknowledgments.** We thank the officers and crew of RRS *Charles Darwin* for their assistance during cruises CD82 and CD108 and, in particular, Tony Watts, who was chief scientist for CD82. These cruises were supported by the Natural Environment Research Council (NERC), UK (grant GR3/8554) and the Southampton Oceanography Centre. The elevation data for El Hierro and Tenerife were originally created by M. J. R. Gee and R. Dalwood [*Dalwood*, 1996; *Gee*, 1999]. Figures in this paper were prepared with the GMT software system [*Wessel and Smith*, 1991]. We thank the reviewers and editors of this paper for helpful and constructive comments. W.B.D. and N.C.M. were supported by research fellowships from the NERC and the Royal Society, respectively.

## References

Ablay, G., and M. Hurlimann, Evolution of the north flank of Tenerife by recurrent giant landslides, *J. Volcanol. Geotherm. Res.*, *103*, 135–159, 2000.

Ancochea, E., J. M. Fuster, E. Ibarrola, A. Cendrero, J. Coello, F. Hernan, J. M. Cantagrel, and C. Jamond, Volcanic evolution of the island of Tenerife (Canary Islands) in the light of new K-Ar data, *J. Volcanol. Geotherm. Res.*, *44*, 231–249, 1990.

Arana, V., A. G. Camacho, A. Garcia, F. G. Montesinos, I. Blanco, R. Vieira, and A. Felpeto, Internal structure of Tenerife (Canary Islands) based on gravity, aeromagnetic and volcanological data, *J. Volcanol. Geotherm. Res.*, *103*, 43–64, 2000.

Cantagrel, J. M., N. O. Arnaud, E. Ancochea, J. M. Fuster, and M. J. Huertas, Repeated debris avalanches on Tenerife and genesis of La Canada caldera wall (Canary Islands), *Geology*, *27*, 739–742, 1999.

Carey, S., T. Maria, and W. Cornell, Processes of volcaniclastic sedimentation during the early growth stages of Gran Canaria based on sediments from Site 953, *Proc. Ocean Drill. Program Sci. Results*, *157*, 183–200, 1998.

Carracedo, J. C., The Canary Islands: An example of structural control on the growth of large oceanic-island volcanoes, *J. Volcanol. Geotherm. Res.*, *60*, 225–241, 1994.

Carracedo, J. C., S. Day, H. Guillou, E. Rodriguez Badiola, J. A. Canas, and F. J. Perez Torrado, Hotspot volcanism close to a passive continental margin: The Canary Islands, *Geol. Mag.*, *135*, 591–604, 1998.

Carracedo, J. C., S. J. Day, H. Guillou, and F. J. Perez Torrado, Giant Quaternary landslides in the evolution of La Palma and El Hierro, Canary Islands, *J. Volcanol. Geotherm. Res.*, *94*, 169–190, 1999.

Clague, D. A., and G. B. Dalrymple, Tectonics, geochronology, and origin of the Hawaiian-Emperor volcanic chain, in *The Geology of North America,* vol. N, *The Eastern Pacific Ocean and Hawaii*, edited by E. L. Winterer, D. M. Hussong, and R. W. Decker, pp. 188–217, Geol. Soc. of Am., Boulder, Colo., 1989.

Dalwood, R. E. T., A seismic study of lithospheric flexure in the vicinity of the Canary Islands, Ph.D. thesis, Univ. of Oxford, Oxford, U.K., 1996.

Farre, J. A., B. A. McGregor, W. B. F. Ryan, and J. M. Robb, Breaching the shelfbreak: Passage from youthful to mature phase in submarine canyon evolution, in *The Shelfbreak: Critical Interface on Continental Margins*, edited by D. J. Stanley and G. T. Moore, *Spec. Publ. SEPM*, *33*, 25–39, 1983.

Funck, T., and H. Lykke-Andersen, Seismic structure of the volcanic apron north of Gran Canaria, *Proc. Ocean Drill. Program Sci. Results*, *157*, 11–28, 1998.
Funck, T., and H.-U. Schmincke, Growth and destruction of Gran Canaria deduced from seismic reflection and bathymetric data, *J. Geophys. Res.*, *103*, 15,393–15,407, 1998.
Gee, M. J. R., The collapse of oceanic islands and the mechanics of long runout debris flows: Examples from the NW African margin, Ph.D. thesis, Univ. of Oxford, Oxford, U.K., 1999.
Gee, M. J. R., D. G. Masson, A. B. Watts, and N. C. Mitchell, Offshore continuation of volcanic rift zones, El Hierro, Canary Islands, *J. Volcanol. Geotherm. Res.*, *105*, 107–119, 2001.
Guillou, H., J. C. Carracedo, F. Perez-Torado, and E. Rodriguez Badiola, K-Ar ages and magnetic stratigraphy of a hotspot-induced, fast-grown oceanic island: El Hierro, Canary Islands, *J. Volcanol. Geotherm. Res.*, *73*, 141–155, 1996.
Hammerstad, E., F. Pohner, F. Parthiot, and J. Bennett, Field testing of a new deep water multibeam echo sounder, in *Oceans '91*, pp. 743–749, Inst. of Electr. and Electr. Eng., New York, 1991.
Hartshorn, K., N. Hovius, W. B. Dade, and R. L. Slingerland, Climate-driven bedrock incision in an active mountain belt, *Science*, *297*, 2036–2038, 2002.
Hooghiemstra, H., Variations of the NW African trade wind regime during the last 140,000 years: Changes in polen flux evidenced by marine sediment records, in *Paleoclimatology and Paleometeorology: Modern and Past Patterns of Global Atmospheric Transport*, edited by M. Leinen and M. Sarnthein, pp. 733–770, Kluwer Acad., Norwell, Mass., 1989.
Krastel, S., H.-U. Schmincke, and C. L. Jacobs, Formation of submarine canyons on the flanks of the Canary Islands, *Geo Mar. Lett.*, *20*, 160–167, 2001a.
Krastel, S., H.-U. Schmincke, C. L. Jacobs, R. Rihm, T. P. Le Bas, and B. Alibes, Submarine landslides around the Canary Islands, *J. Geophys. Res.*, *106*, 3977–3997, 2001b.
Marlow, M. S., J. V. Gardner, and W. R. Normark, Using high-resolution multibeam bathymetry to identify seafloor surface rupture along the Palos Verdes fault complex in offshore southern California, *Geology*, *28*, 587–590, 2000.
Masson, D. G., Catastrophic collapse of the volcanic island of Hierro 15 ka ago and the history of landslides in the Canary Islands, *Geology*, *24*, 231–234, 1996.
Masson, D. G., A. B. Watts, M. J. R. Gee, R. Urgeles, N. C. Mitchell, and T. P. Le Bas, Slope failures on the flanks of the western Canary Islands, *Earth Sci. Rev.*, *57*, 1–35, 2002.
Menard, H. W., Insular erosion, isostasy, and subsidence, *Science*, *220*, 913–918, 1983.
Michelchen, N., Estimates of large-scale atmospheric pressure variations in the upwelling area off Northwest Africa, in *Coastal Upwelling*, *Coast. Estuar. Sci*., vol. 1, edited by F. Richard, pp. 17–20, AGU, Washington, D. C., 1981.
Mitchell, N. C., A model for attenuation of backscatter due to sediment accumulations and its application to determine sediment thickness with GLORIA side–scan sonar, *J. Geophys. Res.*, *98*, 2477–2493, 1993.
Mitchell, N. C., D. G. Masson, A. B. Watts, M. J. R. Gee, and R. Urgeles, The morphology of the flanks of volcanic ocean islands: A comparative study of the Canary and Hawaiian hotspot islands, *J. Volcanol. Geotherm. Res.*, *115*, 83–107, 2002.
Montgomery, D. R., Valley incision and the uplift of mountain peaks, *J. Geophys. Res.*, *99*, 13,913–13,921, 1994.
Montgomery, D. R., and H. M. Greenberg, Local relief and the height of Mount Olympus, *Earth Surf. Proc. Landforms*, *25*, 385–396, 2000.
Pratson, L. F., and B. J. Coakley, A model for the headwall erosion of submarine canyons induced by downslope-eroding sediment flows, *Geol. Soc. Am. Bull.*, *108*, 225–234, 1996.
Pratson, L. F., W. B. F. Ryan, G. S. Mountain, and D. C. Twichell, Submarine canyon initiation by downslope-eroding sediment flows: Evidence in late Cenozoic strata on the New Jersey continental slope, *Geol. Soc. Am. Bull.*, *106*, 395–412, 1994.
Rodriguez-Losada, J. A., J. Martinez-Frias, M. A. Bustillo, A. Delgado, A. Hernandez-Pacheco, and J. V. de la Fuente Krauss, The hydrothermally altered ankaramite basalts of Punta Poyata (Tenerife, Canary Islands), *J. Volcanol. Geotherm. Res.*, *103*, 367–376, 2000.
Sarnthein, M., J. Thiede, U. Pflaumann, H. Erlenkeuser, D. Futterer, B. Koopmann, H. Lange, and E. Seibold, Atmospheric and oceanic circulation patterns of northwest Africa during the past 25 million years, in *Geology of the Northwest African Continental Margin*, edited by U. von Rad et al., pp. 545–603, Springer-Verlag, New York, 1982.
Schmincke, H.-U., and M. Sumita, Volcanic evolution of Gran Canaria reconstructed from apron sediments: Synthesis of VICAP project drilling, *Proc. Ocean Drill. Program Sci. Results*, *157*, 443–469, 1998.
Schmincke, H.-U., et al., Background, objectives, and principal results of drilling the clastic apron of Gran Canaria (VICAP), *Proc. Ocean Drill. Program Initial Rep.*, *157*, 11–25, 1995.
Schneider, J.-L., C. A. Brunner, and S. Kuttner, Epiclastic sedimentation during the upper Miocene-lower Pliocene volcanic hiatus of Gran Canaria: Evidence from Sites 953 and 954, *Proc. Ocean Drill. Program Sci. Results*, *157*, 293–313, 1998.
Selby, M. J., *Hillslope Materials and Processes*, 451 pp., Oxford Univ. Press, Oxford, U.K, 1993.
Teide Group, Morphometric interpretation of the northwest and southeast slopes of Tenerife, Canary Islands, *J. Geophys. Res.*, *102*, 20,325–20,342, 1997.
Thirlwall, M. F., B. S. Singer, and G. F. Marriner, $^{39}$Ar-$^{40}$Ar ages and geochemistry of the basaltic shield stage of Tenerife, Canary Islands, Spain, *J. Volcanol. Geotherm. Res.*, *103*, 247–297, 2000.
Tucholke, B. E., W. K. Stewart, and M. C. Kleinrock, Long-term denudation of ocean crust in the central North Atlantic Ocean, *Geology*, *25*, 171–174, 1997.
Urgeles, R., M. Canals, J. Baraza, B. Alonso, and D. G. Masson, The most recent megaslides on the Canary Islands: The El Golfo Debris Avalanche and the Canary Debris Flow, west El Hierro Island, *J. Geophys. Res.*, *102*, 20,305–20,323, 1997.
Urgeles, R., D. G. Masson, M. Canals, A. B. Watts, and T. Le Bas, Recurrent large-scale landsliding on the west flank of La Palma, Canary Islands, *J. Geophys. Res.*, *104*, 25,331–25,348, 1999.
Vogt, P. R., and N. C. Smoot, The Geisha Guyots: Multi-beam bathymetry and morphometric interpretation, *J. Geophys. Res.*, *89*, 1085–1107, 1984.
Watts, A. B., and D. G. Masson, A giant landslide on the north flank of Tenerife, Canary Islands, *J. Geophys. Res.*, *100*, 24,499–24,507, 1995.
Watts, A. B., and D. G. Masson, New sonar evidence for recent catastrophic collapses of the north flank of Tenerife, Canary Islands, *Bull. Volcanol.*, *63*, 8–19, 2001.
Watts, A. B., C. Peirce, J. Collier, R. Dalwood, J. P. Canales, and T. J. Henstock, A seismic study of lithospheric flexure in the vicinity of Tenerife, Canary Islands, *Earth Planet. Sci. Lett.*, *146*, 431–447, 1997.
Wessel, P., and W. H. F. Smith, Free software helps map and display data, *Eos Trans. AGU*, *72*, 441, 445–446, 1991.

---

W. B. Dade, Department of Earth Sciences, Fairchild Hall HB 6105, Dartmouth College, Hanover, NH 03755, USA. (W.Brian.Dade@dartmouth.edu)

D. G. Masson, Challenger Division, Southampton Oceanography Centre, European Way, Southampton SO14 3ZH, UK. (dgm@soc.soton.ac.uk)

N. C. Mitchell, Department of Earth Sciences, Cardiff University, P.O. Box 914, Cardiff CF10 3YE, UK. (neil@ocean.cf.ac.uk)